CHAPTER 11

Waves and Their Impact on Reef Growth

Curt D. Storlazzi[1], Michael E. Field[1], Eric K. Brown[2], and Paul L. Jokiel[3]

It has been known for some time that there are strong qualitative correlations between wave energy and coral distribution (Rosen, 1975; Geister, 1977; Vosburgh, 1977; Dollar, 1982; Done, 1983; Massel and Done, 1993; Rogers, 1993; Blanchon and Jones, 1997). Grigg (1998) has most recently discussed the interplay between wave energy and reef properties in the Hawaiian Islands, but as in most past studies, wave-energy is classified in terms of the loosely divided categories of "low," "medium," and "high" wave energy regimes. Jokiel and others (2004) show that maximum wave height in Hawai'i is negatively correlated with coral cover, diversity, and species richness. There has yet to be, however, a large-scale quantitative investigation of these relationships that compares the motions exerted by waves upon the reef to the distribution of different stony coral species. Our goal here is to better quantify the interplay between wave-induced forces, reefs, and corals.

Waves

Wave Observations and Modeling

In order to provide accurate wave data for the entire south shore of Moloka'i, we used the U.S. Naval Oceanographic Office's Spectral Wave Prediction System (SWAPS) version 4.0 wave model (Storlazzi and others, 2005). This model generated a gridded field of wave height, wave period, and wave direction for analysis. Real-time output of wave height and wave period were compared to concurrent observations of wave height and wave period made at two U.S. National Oceanographic and Atmospheric Administration (NOAA) offshore deep-water buoys (#51001 and #51002; National Data Buoy Center, 2002) and five wave/tide gauges that we deployed in 11-m (36 ft) mean water depth off the south shore of Moloka'i (fig. 1). Wave heights and wave periods calculated from the wave model differed from the measurements by less than 10 percent and verified that the model's estimation of energy loss due to refraction and shoaling worked properly. The modeled wave heights and wave periods produced by the wave model for the shallowest grid cells that were closest to the south shore of Moloka'i were then used for input into the coral force-balance model. When the orbital motion of the water as a wave passes interacts with the sea floor, it imparts a force or stress (stress = force/area) on the sea floor; this stress is better known as a wave-induced shear stress. Table 1 gives examples of how variations in wave height, wave period, and water depth affect wave-induced shear stresses on the sea floor. These peak wave-induced near-bed shear stresses were calculated following the methodology presented by Jonsson (1966).

[1] U.S. Geological Survey Pacific Science Center, 400 Natural Bridges Dr., Santa Cruz, CA 95060

[2] University of Hawai'i, Hawai'i Institute of Marine Biology, P.O. Box 1346, Kaneohe, HI 96744; current address: Kalaupapa National Historical Park, P.O. Box 2222, Kalaupapa, HI 96742

[3] University of Hawai'i, Hawai'i Institute of Marine Biology, P.O. Box 1346, Kane'ohe, HI 96744

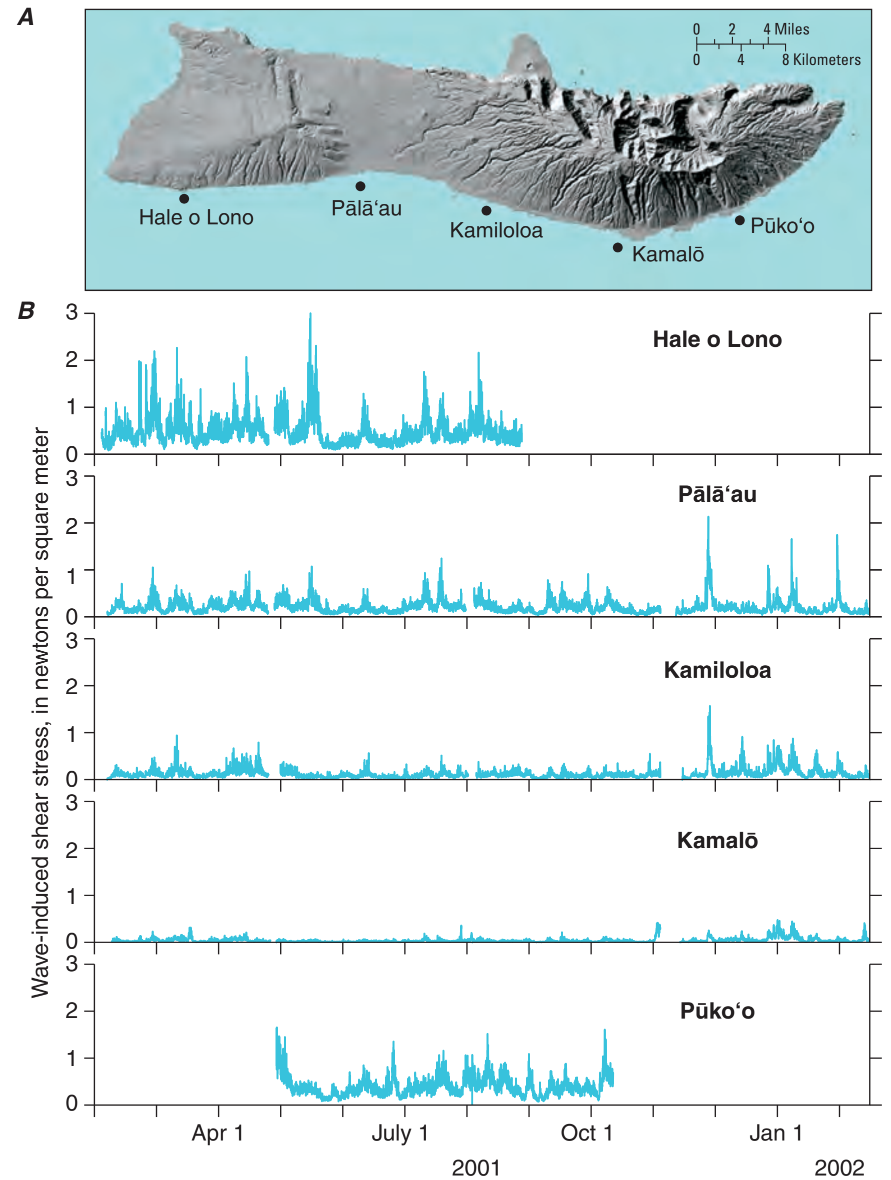

Figure 1. U.S. Geological Survey (USGS) wave data for south coast of Moloka'i. *A.*, Location of USGS wave and tide gauges deployed along the 11-m (36-ft) isobath. *B*, Calculated peak wave-induced near-bed shear stresses from the USGS wave and tide gauges. Gaps in the individual gauges' records are a result of instrument failures.

Table 1. Examples of variations in wave-induced shear stresses caused by variations in wave height, wave period, and water depth.
[Peak wave-induced near-bed shear stresses calculated as per Jonsson (1966)]

Variable	Wave height (m)	Wave period (s)	Water depth (m)	Resulting shear stress (N/m^2)
	1	10	15	0.42
Wave height	2	10	15	1.36
	3	10	15	2.72
	1	5	15	0.04
Wave period	1	10	15	0.42
	1	15	15	0.54
	1	10	5	1.38
Water depth	1	10	15	0.42
	1	10	25	0.20

The wave events modeled corresponded to the largest waves observed for each wave-energy regime over the previous 15 years for which the boundary-condition data were of a high enough quality to run the wave model (table 2). We chose to use these events because 15 years approaches the recovery time for the dominant coral species observed off Moloka'i (Dollar, 1982; Grigg, 1983) and corals and their resulting reefs generally develop under the environmental conditions observed over the time necessary for their recovery (Graus and others, 1984; Rogers, 1993). The North Pacific swell model run displayed a strong shadowing effect by the island of Moloka'i along its south coast (fig. 2). The north, east, and west sides of the island were exposed to the brunt of this large swell, which could generate peak wave-induced near-bed shear stresses greater than 1.75 N/m^2 (newtons per square meter) along most of Moloka'i's shoreline. The area off the south

Table 2. Modeled wave conditions.
[Based on data from the National Data Buoy Center (2002)]

Wave regime	Date (month/day/year)	Wave height (m)	Wave period (s)	Wave direction from (deg)	Wind speed (m/s)
North Pacific swell	01/28/1998	8.4	20	320	6.1
Trade-wind waves	06/23/1998	3.2	8	50	13.8
Southern Ocean swell	06/08/2000	2.5	20	180	6.2

shore, which contains the large fringing reef, is a shadow zone for North Pacific swell, with modeled peak wave-induced near-bed shear stresses less than 0.25 N/m^2. Along most of the fringing reef, these peak stresses were less than 0.10 N/m^2 in 10 m (33 ft) of water. At both the east and west ends of the island, where the reef narrows, peak wave-induced near-bed shear stresses rapidly increase fivefold to more than 0.50 N/m^2 as some wave energy refracts around the ends of the island (fig. 3).

Kona storm waves (not shown), which were modeled to observe how the south shore of Moloka‘i would be affected by an unrefracted swell from the south, did not generate high near-bed wave orbital velocities (peak wave-induced near-bed shear stresses = 0.08 N/m^2) anywhere along the island. The Southern Ocean swell, on the other hand, produced intermediate values of peak wave-induced near-bed shear stresses (~0.25 N/m^2) along almost the entire length of Moloka‘i’s fringing reef, and these waves have been observed to resuspend high quantities of fine-grained terrestrial sediment on the reef flat (Storlazzi and others, 2000). The modeled northeast trade-wind waves appear to affect primarily the east and southeast coast of the island. The coastline between the southernmost point of the island at Kamalō and the east end of the island is directly exposed to trade-wind waves. This resulted in peak wave-induced near-bed shear stresses being 50 percent to 100 percent higher than to the west of Kamalō, where the coast is protected from direct impact of trade-wind waves. The short wave period characteristic of trade-wind waves is reflected in the greater disparity between the peak wave-induced near-bed shear stresses for the different isobaths east of Kamalō than to the west of Kamalō, where the coastline is not directly affected by these waves (fig. 4). These waves produce rather low values of peak wave-induced near-bed shear stresses to the west of Kamalō, on the order of 0.15 N/m^2. However, the modeling suggests that trade-wind waves, in combination with a typical North Pacific swell, can generate much higher peak wave-induced near-bed shear stresses along the east and southeast shore of Moloka‘i, on the order of 0.40–0.50 N/m^2, in the area where the reef starts to pinch out.

Figure 3. Aerial photograph looking north over Moloka‘i’s west end, showing North Pacific winter swell waves wrapping around Lā‘au Point and propagating east along the southwest shore.

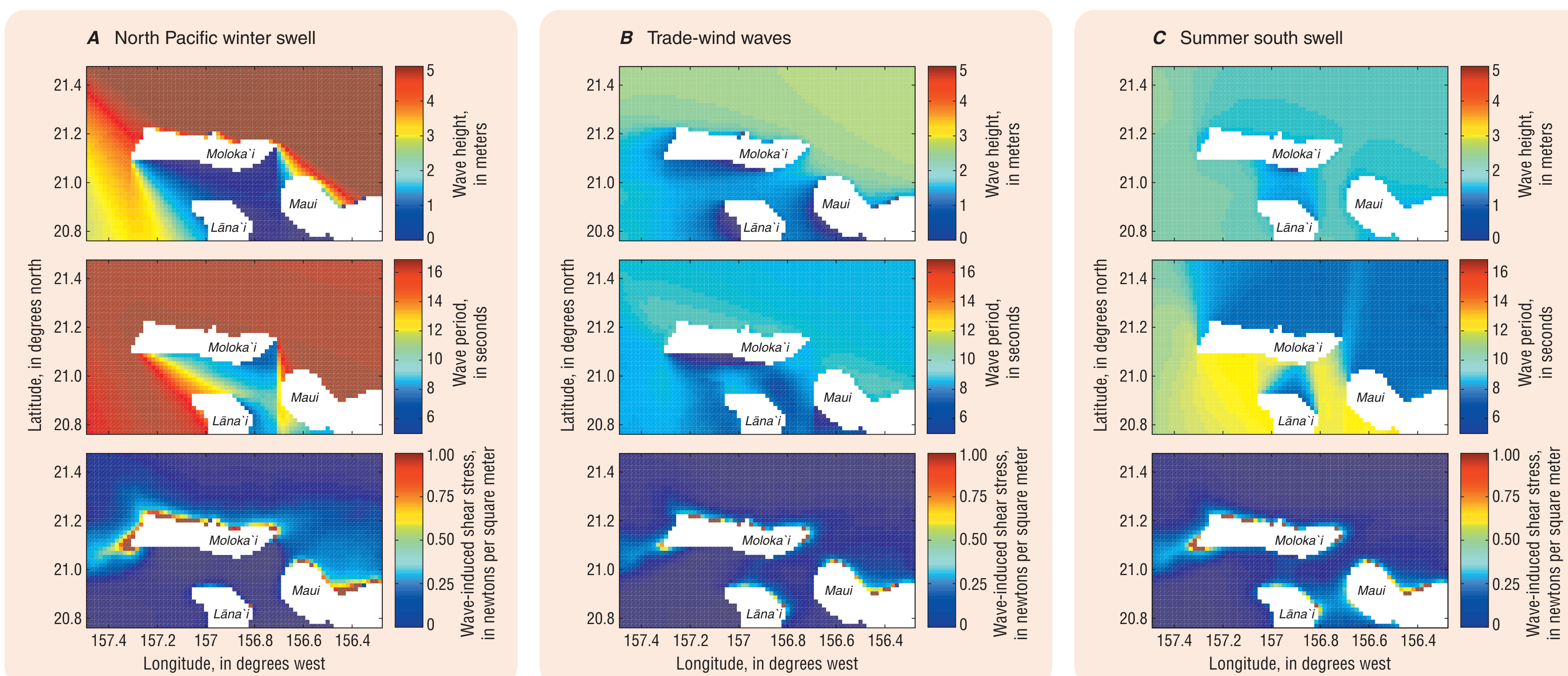

Figure 2. Wave model runs for three of the main wave climates for Moloka‘i. Note how the different combinations of wave heights, wave periods, and wave directions result in different areas being affected by high peak wave-induced near-bed shear stresses. *A*, North Pacific winter swell. *B*, Trade-wind waves. *C*, Summer south swell.

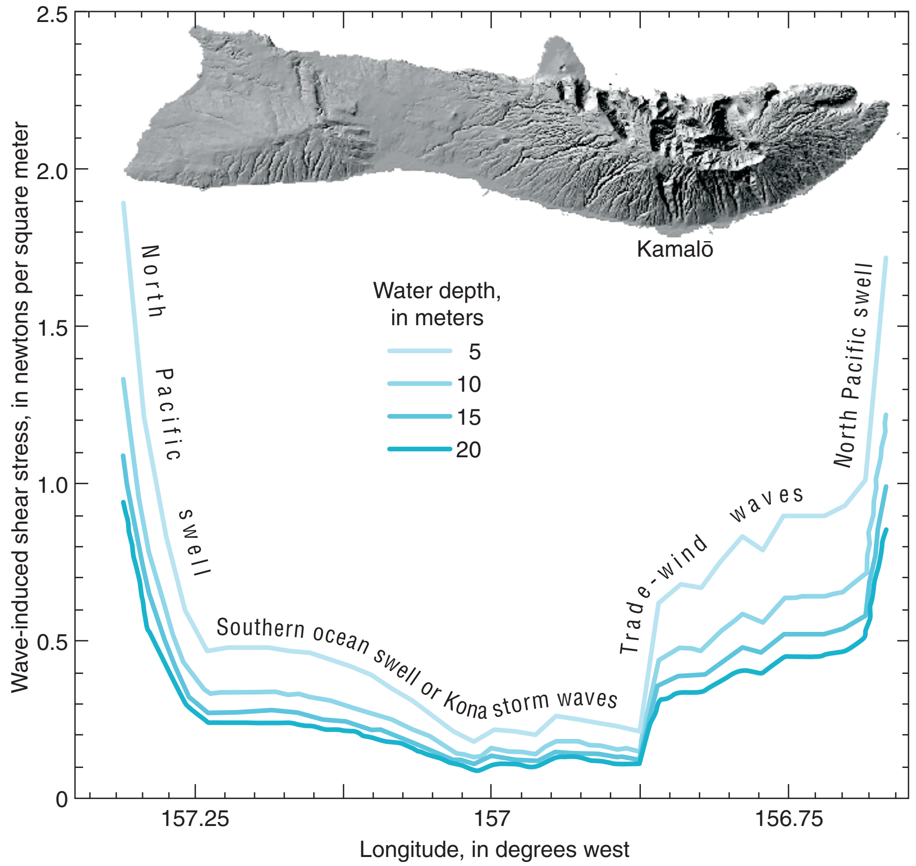

Figure 4. Modeled peak wave-induced near-bed shear stresses at different depths off Moloka‘i’s south shore. Also noted are the different types of waves that dominate each section of coastline.

Relationship Between Waves and Reef Morphology

Overall Reef Morphology

A strong inverse exponential relationship ($r^2 > 0.81$) exists between the modeled peak wave-induced near-bed shear stresses and the width of the reef flat at different locations along the south shore of Moloka‘i (fig. 5). This correlation implies that reef-flat width, and thus very likely the overall reef width, decreases exponentially with increasing wave energy.

Spur-and-Groove Morphology

Computed mean spur heights and spur widths for the south Moloka‘i reef were compared to the modeled wave-induced peak bed shear stresses to determine if there are any relations between spur-and-groove morphology and wave forces. Mean spur height along the 5-m, 10-m, 15-m and 20-m (16-ft, 33-ft, 49-ft, and 66-ft) isobaths was shown to decrease logarithmically with increasing modeled peak wave-induced near-bed shear stresses (fig. 6*A*). Mean spur width along the same four isobaths showed a similar relation to wave energy, decreasing logarithmically with increasing peak wave-induced near-bed shear stresses (fig. 6*B*). However, at shallow depths (5 m), spur height and spur width both displayed a trend opposite to the data for the four isobaths, with a slight increase in height or width with increasing peak wave-induced near-bed shear stresses (not shown).

The ratio of spur height to spur width decreased logarithmically with increasing peak wave-induced near-bed shear stresses (fig. 6*C*); this relation is significant above the 1-percent level. The low percentages of variability indicated by these correlations between waves and spur-and-groove morphology are likely due to a number of factors. These include natural variability in a complex biogeomorphological system, the disproportionate spatial resolutions of the SHOALS data (on the order of meters) and the wave model output (on the order of kilometers), and other important controls like variations in light availability for photosynthesis due to turbidity.

Spur-and-groove features appeared to occur in two distinctly different morphological groups correlated with different wave energies (fig. 7). Overall, spur-and-groove structures tended to be more than twice as high (1.1 m or 3.6 ft) and slightly wider (93 m or 305 ft) in lower energy environments as compared to those in higher energy environments (0.5 m and 87 m, or 1.6 ft and 285 ft, respectively). In regions of low wave energy, numerous short, narrow spur-and-groove structures are observed in shallow water depths (fig. 7*B*), whereas in mid water depths (fig. 7*C*), fewer, broader, and taller spurs dominated, followed by a reversal back to more numerous, short and narrow spurs lower on the fore reef along the 20-m isobath. The numerous short, narrow spur-and-groove structures either truncated or merge together to form the fewer, broader and taller spur-and-groove structures along the 15-m isobath.

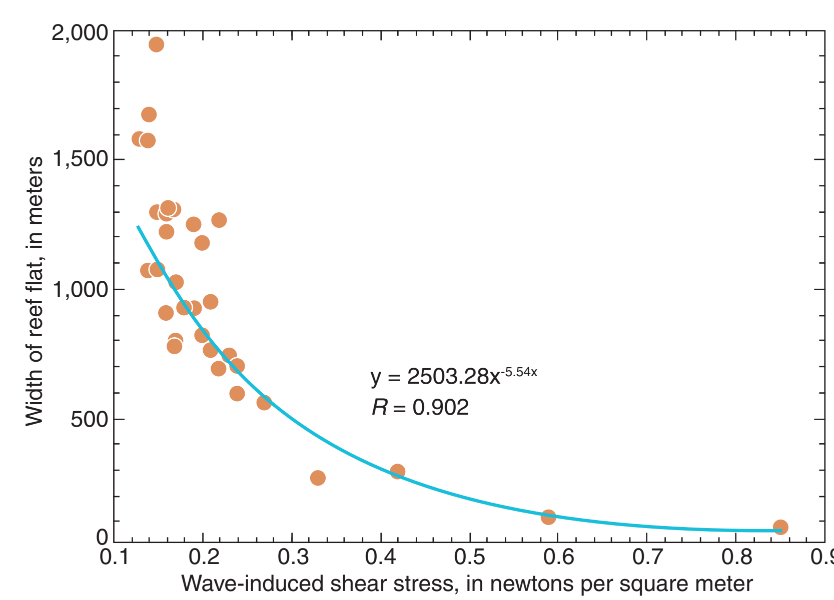

Figure 5. Plot showing the relation between peak wave-induced near-bed shear stress and the width of the reef flat off Moloka‘i’s south shore. The exponential curve fit is significant above the 0.1-percent level. This trend demonstrates that the reef flat is widest where the wave energy is lowest.

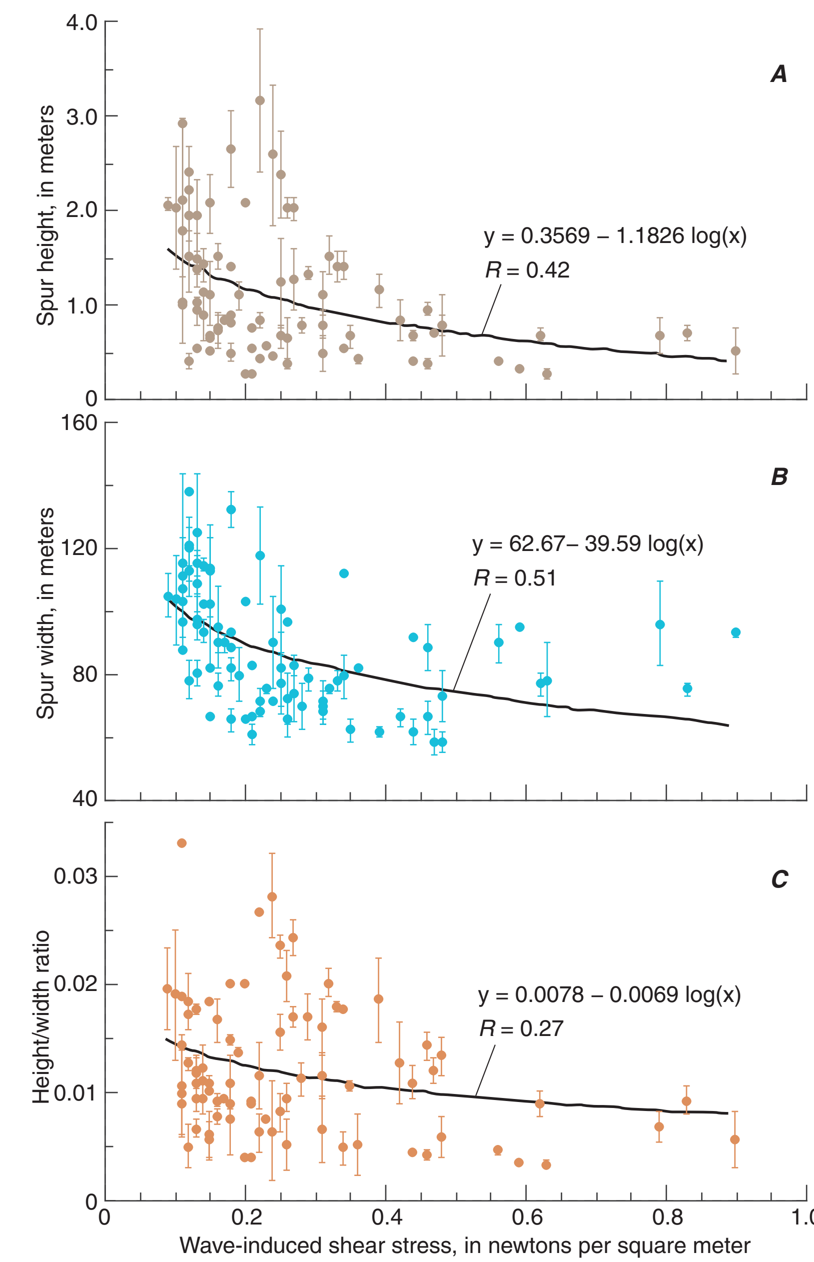

Figure 6. Relations between peak wave-induced near-bed shear stress and shape parameters of coral spurs: spur height (*A*), spur width (*B*), and ratio of spur height to spur width (*C*). The error bars denote ± one standard deviation. The exponential curve fits in *A*, *B*, and *C* are significant above the 0.1-percent, 0.1-percent, and 2-percent levels, respectively. Spur height and width are variable, but spurs tend to be higher and wider at low wave-induced shear stresses and become shorter and narrower at high shear stresses. The data suggest that waves are the dominant factor controlling spur-and-groove morphology, but they explain only a relatively low percent of the variability. Natural variability in the system and other factors, such as light availability for photosynthesis, turbidity, and the high resolution of the measurements as compared to the low spatial resolution of the wave model, are likely other sources of variability.

In higher energy environments, however, spur-and-groove structures tended to be roughly similar in height and width regardless of water depth, with the tallest spurs typically being observed in the shallowest water depths (fig. 7*D–E*). The spur-and-groove measurements in shallow water (5 m) agree with the observations made by Munk and Sargent (1954) along atolls in the western Pacific Ocean and by Roberts (1974) along Grand Cayman in the Caribbean Sea. At greater depths (15–20 m or 49–66 feet) off Moloka‘i, the relation of spur-and-groove morphology to wave energy was the exact opposite of that found by Roberts and others (1980) and Blanchon and Jones (1997) along the deeper shelf-edge reef off Grand Cayman. The population of reef-forming corals in both the Caribbean and western Pacific is distinctly different from those of Hawai‘i. It is not clear what role different species may play in influencing the morphology of spur-and-groove structures.

Implications of Results to Understanding Processes of Reef Formation

The relations shown here between modeled wave parameters and reef morphology suggest that peak wave-induced near-bed shear stresses are a dominant control on the distribution and morphology of the reef off southern Moloka‘i. The central portion of the reef is protected from the direct impact by large waves, and thus the reef framework is able to develop into an extensive shallow reef flat and broad fore reef. The east and west ends of the island are exposed to larger, longer period waves that generate high orbital wave velocities and thus strong near-bed shear stresses. This appears to limit substantial reef development because of physical breakage of the coral and high abrasion by both bedload and suspended sediment (Dollar, 1982; Grigg, 1998).

In order to explain the variability in spur-and-groove morphology at a given water depth, where light availability remains relatively constant, other physical factors must come into play (fig. 7). The slightly higher and more widely spaced spurs in higher energy shallow areas (fig. 7*D*) relative to lower energy shallow regions (fig. 7*B*) may be explained by the interaction between sediment and coral. The spurs in the shallow, high-energy portions of the reef are likely constructed in part by the binding of coral rubble by diagenetic cementation or coralline algae as described by Shinn and others (1981), Macintyre (1997) and Rasser and Riegl (2002). These studies and others (Tribble and others, 1990, 1992; Brainthwaite and others, 2000) have shown that such processes are dominant along low-slope energetic shallow reef crests and upper fore reefs but are absent along the more quiescent deeper portions of the steep fore reef. The large amount of coral rubble and coarse-grained sediment resulting from the weathering of broken coral may effectively increase the abrasion experienced by corals closer to the sea bed. Consequently only those spurs with enough height to avoid this abrasion likely promote coral growth. Thus, higher wave energy in more exposed shallow areas may advance spur development through cementation and binding of coral rubble, whereas at depth intact coral development may be retarded by wave stresses where these processes are absent and in-place coral growth dominates.

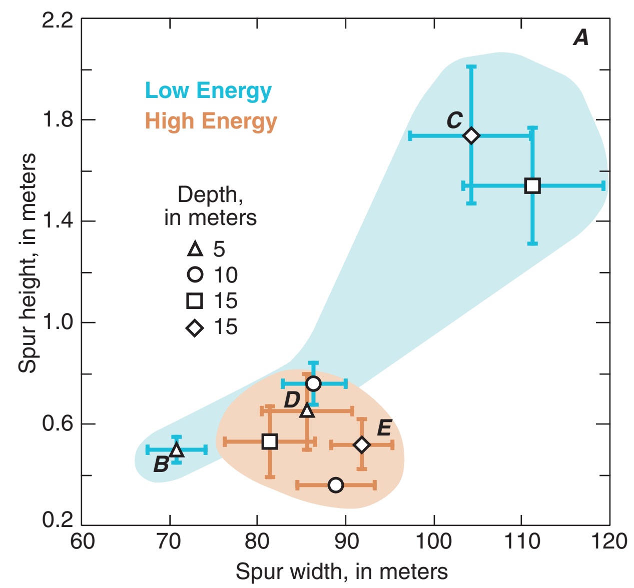

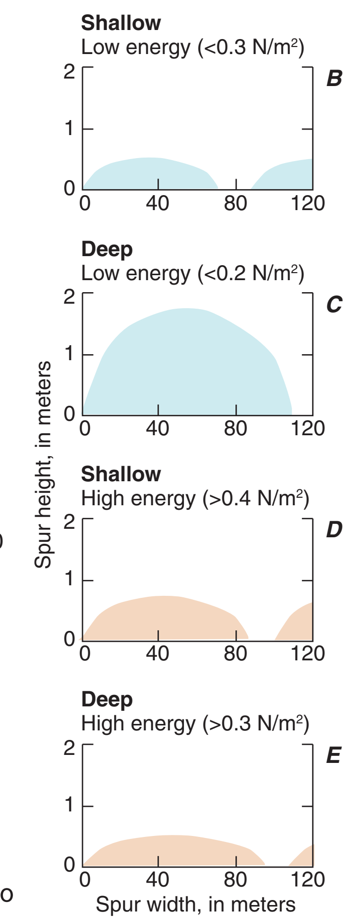

Figure 7. Diagrams showing the relations among spur morphology, wave energy, and water depth off south Moloka‘i. *A*, Plot of spur width against spur height in different conditions. The error bars denote ±one standard deviation. *B–E*, Cross-sectional profiles of typical spurs at different water depths and levels of wave energy. In low-energy conditions, the spurs are short and narrow in shallow water (*B*) but are very tall and wide in deeper water (*C*). In high-energy areas, by contrast, the spurs do not vary much in shape (*D–E*), suggesting that different processes might be more important in defining coral-spur morphology in calm areas versus high-energy areas.

Another significant factor shown to control reef development is antecedent topography. While a lower gradient shelf would result in a greater cross-shore extent of the shelf being situated in the zone optimal for coral growth in terms of light availability and wave energy, reef development in this space would still be contingent on low enough wave energy to allow reef growth. This is why well-developed active reefs are not observed off northern O‘ahu or Maui. These areas have similar coastal configurations to south Moloka‘i but are directly impacted by the large North Pacific swell that generates extremely high (>1.5 N/m^2) peak wave-induced near-bed shear stresses (Grigg, 1998).

These analyses clearly show that waves are the primary control on both large-scale reef morphology and smaller scale spur-and-groove morphology where high peak wave-induced near-bed shear stresses are present. In these areas light, water depth, and antecedent topography are subordinate. The higher morphologic variability at lower peak wave-induced near-bed shear stresses demonstrates that when wave-induced water motions are low enough as to not dominate reef and spur-and-groove morphology, other factors such as light availability for in-place coral growth and the ability to bind or cement rubble increase and may become the dominant factors.

Suggested citation:

Storlazzi, Curt D., Field, Michael E., Brown, Eric K., and Jokiel, Paul L., 2008, Waves and their impact on reef growth, *Chapter 11 of* Field, M.E., Cochran, S.A., Logan, J.B., and Storlazzi C.D., eds., The coral reef of south Moloka`i, Hawai`i; portrait of a sediment-threatened fringing reef: U.S. Geological Survey Scientific Investigations Report 2007-5101, p. 105-108 [http://pubs.usgs.gov/sir/2007/5101/sir2007-5101_chapter11.pdf].